THE "SHAPE FACTOR" IN ESTIMATION OF TUNNEL INFLOWS

Dr Steven E. Pells
Director, Pells Consulting www.pellsconsulting.com.au

INTRODUCTION

An estimate of the quantity of seepage inflows to tunnels is usually made to guide dewatering requirements and to address environmental impacts and regulations. Water inflow into tunnels occurs by seepage through the soil or rock matrix, but in the case of tunnels in rock, seepage is usually dominated at locations where open defects or geological structures are encountered. As the location and nature of defects cannot be known with confidence, an estimate of inflow over sections of a tunnel is usually made by assuming laminar "Darcian" flow through an 'equivalent porous media' (EPM) – that is, seepage through a material that has a permeability representative of the sum of flows through the ground substance and any defects.

Historically the EPM approach to estimate seepage relied upon the usage of flownets – this allows the tunnel geometry and local environment to be reduced to a shape factor 'F'. In this paper it is shown that such a shape factor can also be used to reconcile published equations that are widely used for estimation of tunnel inflow. Additionally, results from modern numerical methods, which can be used to simulate seepage inflows, may also be expressed using the shape factor. Flownets (and most published equations) only represent steady-state conditions. In practice, inflows to tunnels typically decrease over time as the ground formation around the tunnel is drained. Transient numerical simulations can represent this process and can also be reduced into shape factors that change over time. The reduction of all these methods to a shape factor allows easy comparison of various approaches.

FLOWNETS AND THE SHAPE FACTOR "F"

Two examples of flownets representing tunnel inflow are presented in Figure 1. These images provide a graphical solution to the mathematical problem of seepage show by constructing flowlines (solid) and equipotentials (dashed – being lines of equal 'total head') according to a set of rules. (These rules are presented in most hydrogeological and / or geotechnical textbooks and are not repeated here). Figure 1A represents a case where there is a constant water level (phreatic surface) above the tunnel, such as from a shallow lake or river above the tunnel, or in the case of sufficient recharge to maintain a constant water level. Figure 1B represents a case where the phreatic surface is drawn down by seepage into the tunnel.

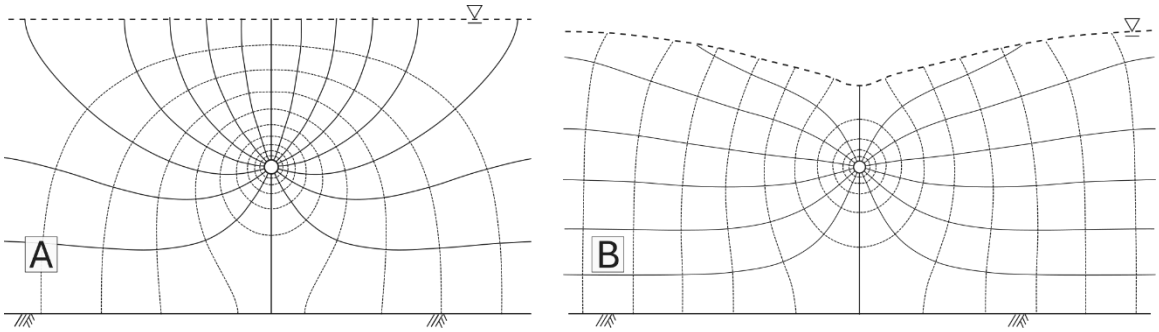

Figure 1 – Examples of flownets: with constant water table (A); with constant lateral boundaries (B). Flow lines are solid and equipotentials are shown as dashed lines.

The seepage discharge 'q' (e.g. in m^3/s per meter length of tunnel) can be calculated according to Equation 1, where: F is a shape factor (dimensionless); k is the hydraulic conductivity (m/s) of the EPM; and, H is the difference in hydraulic total head between the source boundary and the outflow boundary (i.e. the tunnel).

$$q = FkH \tag{1}$$

The shape factor F can be estimated from a flownet as the ratio of the number of flow channels N_f to the number of equipotential "drops" N_d. For example, Figure 1A depicts 16 flow channels with 10 equipotential drops, giving $F = 16/10 = 1.6$. In Figure 1B, $F = 14/11 = 1.27$. However, there is an interesting error here, which only becomes evident with comparison against a numerically generated flownet, discussed below.

PUBLISHED STEADY-STATE INFLOW EQUATIONS AND THE SHAPE FACTOR "F"

Many equations to estimate tunnel seepage have been published. Farhadian and Katibeh (2017) present 10 such equations all of which relate to the "constant phreatic water level" depicted in Figure 1A. In each case the cited equation can be reduced to the form of Equation (1). This is illustrated with five selected equations (r is the tunnel radius):

- Goodman *et al* 1965 $q = 2\pi k \frac{H}{\ln\left(\frac{2H}{r}\right)} \rightarrow F = \frac{2\pi}{\ln\left(\frac{2H}{r}\right)}$ (2)
- Heuer 1995 $q = 2\pi k \frac{H}{8\ln\left(\frac{2H}{r}\right)} \rightarrow F = \frac{2\pi}{8\ln\left(\frac{2H}{r}\right)}$ (3)
- Lei 1999 $q = 2\pi k \frac{H}{\ln\left(\frac{H}{r}+\sqrt{\left(\frac{H}{r}\right)^2-1}\right)} \rightarrow F = \frac{2\pi}{\ln\left(\frac{H}{r}+\sqrt{\left(\frac{H}{r}\right)^2-1}\right)}$ (4)
- Kalsrud 2001 $q = 2\pi k \frac{H}{\ln\left(\frac{2H}{r}-1\right)} \rightarrow F = \frac{2\pi}{\ln\left(\frac{2H}{r}-1\right)}$ (5)
- El-Tani 2003 $q = 2\pi k \frac{\lambda^2-1}{\lambda^2+1}\frac{H}{\ln(\lambda)} \rightarrow F = \frac{2\pi}{\ln(\lambda)}\frac{\lambda^2-1}{\lambda^2+1}$ (6)

  $\lambda = \left(H/r - \sqrt{(H/r)^2-1}\right)$

The shape factor implicit in each of these Equations are plotted in Figure 2A, which allows a rapid comparison of the different values of q that would be yielded from each equation (lines showing 'numerical analysis' are discussed below).

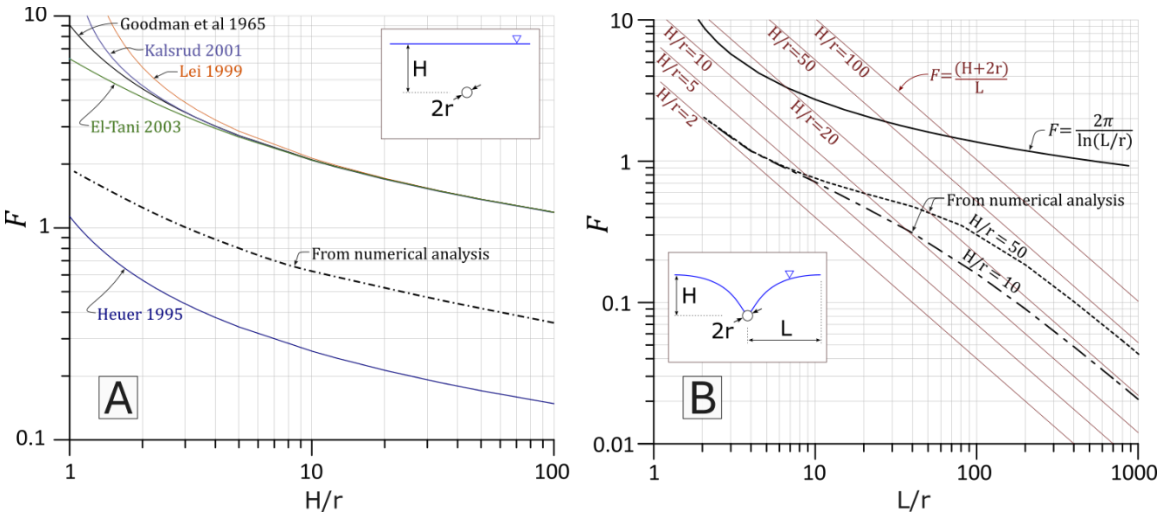

Figure 2 – Comparison of published equations when reduced to a shape factor F

For the case where drawdown exists (e.g. as per Figure 1B), the present author has encountered the usage of Equation (7) in engineering practice, although unfortunately could not find a published source of this equation (L is the horizontal distance from the tunnel to a lateral constant head boundary):

- Unknown $\quad q = 2\pi k \frac{H}{\ln\left(\frac{L}{r}\right)} \quad \rightarrow \quad F = \frac{2\pi}{\ln\left(\frac{L}{r}\right)}$ (7)

Some authors (e.g. Raymer 2005) suggest representing flow to the tunnel as if it were a trench for which the classical Dupuit-Forchheimer expression (Equation 8) applies. Assuming drawdown is to the tunnel crown, this can also be rearranged to yield the following shape factor:

- Dupuit $\quad q_{\text{per side}} = \frac{k}{2L}\left(h_{\text{boundary}} - h_{\text{tunnel}}\right)^2 \quad \rightarrow \quad F = \frac{H+2r}{L}$ (8)
  (i.e. taking $q = 2q_{\text{per side}}$, $H = h_{\text{boundary}} - h_{\text{tunnel}}$ and $h_{\text{tunnel}} = 2r$)

The shape factors implicit in equations relating to a 'drawdown case' are plotted in Figure 2B (again, lines showing 'numerical analysis' are discussed below).

COMMENTS ON THE UTILITY OF THE SHAPE FACTOR "F"

The shape factor reconciles the flownet methodology with various published equations and allows clear comparison between various published methods. In tunnel projects with a specific tunnel radius, depth and / or distance to boundary, it may be pragmatic to communicate in terms of a small range of applicable shape factors (for inflow estimates it may be pragmatic to accept an approximate value for F and focus on reducing uncertainty in the estimate of k).

The shape factor may also be used for other design aspects. For instance, the value of k in Equation (1) may be substituted for the effective hydraulic conductivity k_{eff}, opening the opportunity to assess effects of anisotropy (Equation 9) or of tunnel lining or grouting (Equation 10) on flows for given shape factors.

In the case of anisotropy: $\quad k_{\text{eff}} \cong \frac{k_h + k_v}{2}$ (9)

For the case of a liner (or grouted annulus) of thickness t and conductivity k_{liner}:

$$k_{\text{eff}} = \frac{L}{\frac{t}{k_{\text{liner}}} + \frac{L-t}{k}} \quad (10)$$

A common method of estimating tunnel inflows during construction is to observe inflows from a long, small-diameter pilot hole advanced into the tunnel face. By adopting a shape factor for the probe hole (F_{probe}) the total seepage flow (Q_{probe}) into a pilot hole of length L_{probe} could be estimated using Equation (11). Substitution of Equation (11) into Equation (1) (and assuming a common k and H apply to both tunnel and probe) gives Equation (12) which provides an estimate of tunnel inflow without requiring knowledge of k.

$$Q_{\text{probe}} = F_{\text{probe}}\, kHL_{\text{probe}} \quad (11)$$

$$q_{\text{tunnel}} = \frac{F_{\text{tunnel}}}{F_{\text{probe}}} \frac{Q_{\text{probe}}}{L_{\text{probe}}} \quad (12)$$

NUMERICAL SIMULATION OF THE SHAPE FACTOR "F" FOR STEADY-STATE INFLOWS

Numerical (i.e. finite element or finite difference) modelling of seepage requires input of a k value and boundary conditions and will report a seepage discharge q. These values can be substituted into Equation (1) to yield a numerically derived shape factor F. For example, the

geometry in Figure 3 represents the 'constant phreatic surface' example of Figure 1A and was solved for various water level elevations relative to tunnel diameter to report F as a function of H/r. Similarly, the geometry in Figure 4 represents the "drawdown" case in Figure 1B and was solved for various boundary locations relative to tunnel diameter to report F as a function of L/r. The results from these numerical analyses are included in Figures 2A and 2B, respectively.

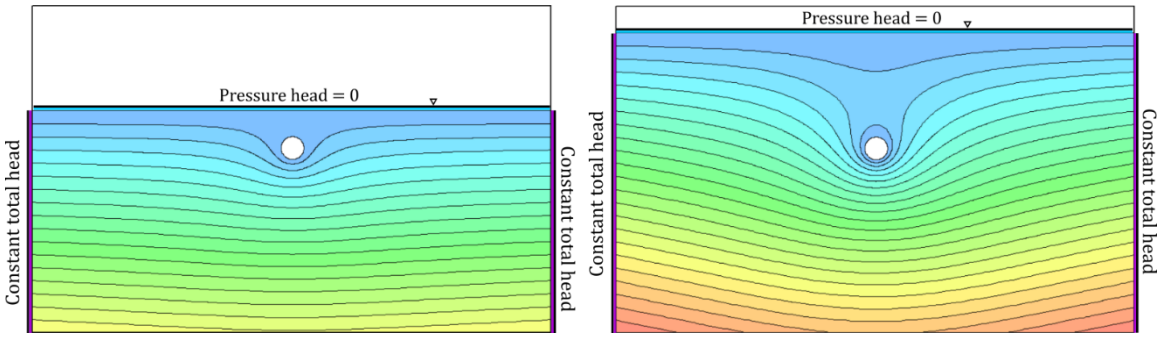

Figure 3 – Illustration of steady-state numerical simulation of constant water table cases – varying depth to water table "H"

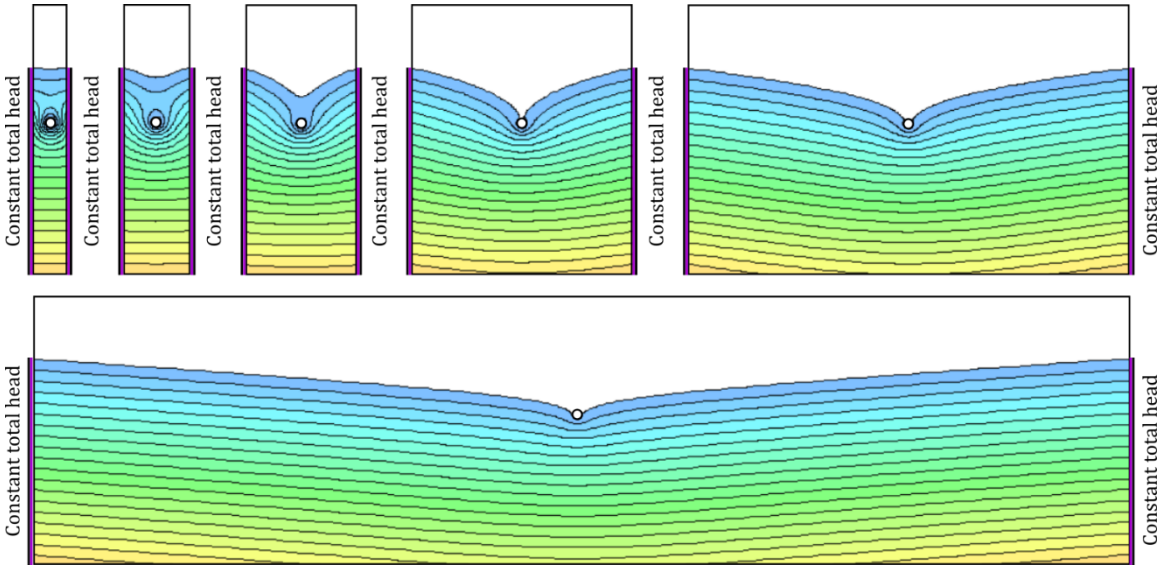

Figure 4– Illustration of steady-state numerical simulation of constant lateral boundaries – varying distance to the boundary "L"

This analysis shows that:

1. Numerically derived steady state F values are generally lower than their analytically derived counterparts. It is interesting that when zooming in to the numerical results, there are many more equipotential lines clustering around the tunnel interface than could be hand-drawn in a graphical flownet approach. For the case of Figure 1A, for instance, when zooming in there are 16 equipotential drops (not 10 as reported above) making the shape factor =1.0, not 1.6. That is, in the numerical model there is increasing head losses at the tunnel interface. It is noted that the numerical modelling utilised here incorporated unsaturated flow mechanics – the reduction of k with desaturation is a relevant phenomenon that should be heeded in tunnel design, but its discussion is beyond the scope of this present paper.

2. Equation (7) does not include a necessary representation of H and appears to have better validity for deeper tunnels. Equation (8) assumes drawdown is to the tunnel crown, which (as seen in Figure 1B and Figure 4) is not necessarily the case. Equation (8) has better validity where the boundary is very distant relative to tunnel diameter.

NUMERICAL SIMULATION OF THE SHAPE FACTOR "F" FOR TRANSIENT INFLOWS

Numerical methods can simulate the development of drawdown over time, and the corresponding reduction in inflows over time, as is observed in tunnelling projects. The geometry in Figure 4 was solved through time for various boundary depths relative to tunnel diameter and for 4 cases of material properties as listed in Table 1. The resulting shape factors, through time, are presented in Figure 5. The decrease of the shape factor over time relates to the decreasing hydraulic gradient toward the tunnel as depressurisation propagates away from the tunnel. In many tunnelling projects there are constraints on inflow tolerated during construction as well as environmental criteria that must be achieved by 'handover'. Hence shape factors both at the time of excavation, and at the time of handover, are of interest, and can be substantially different, as illustrated in Figure 5.

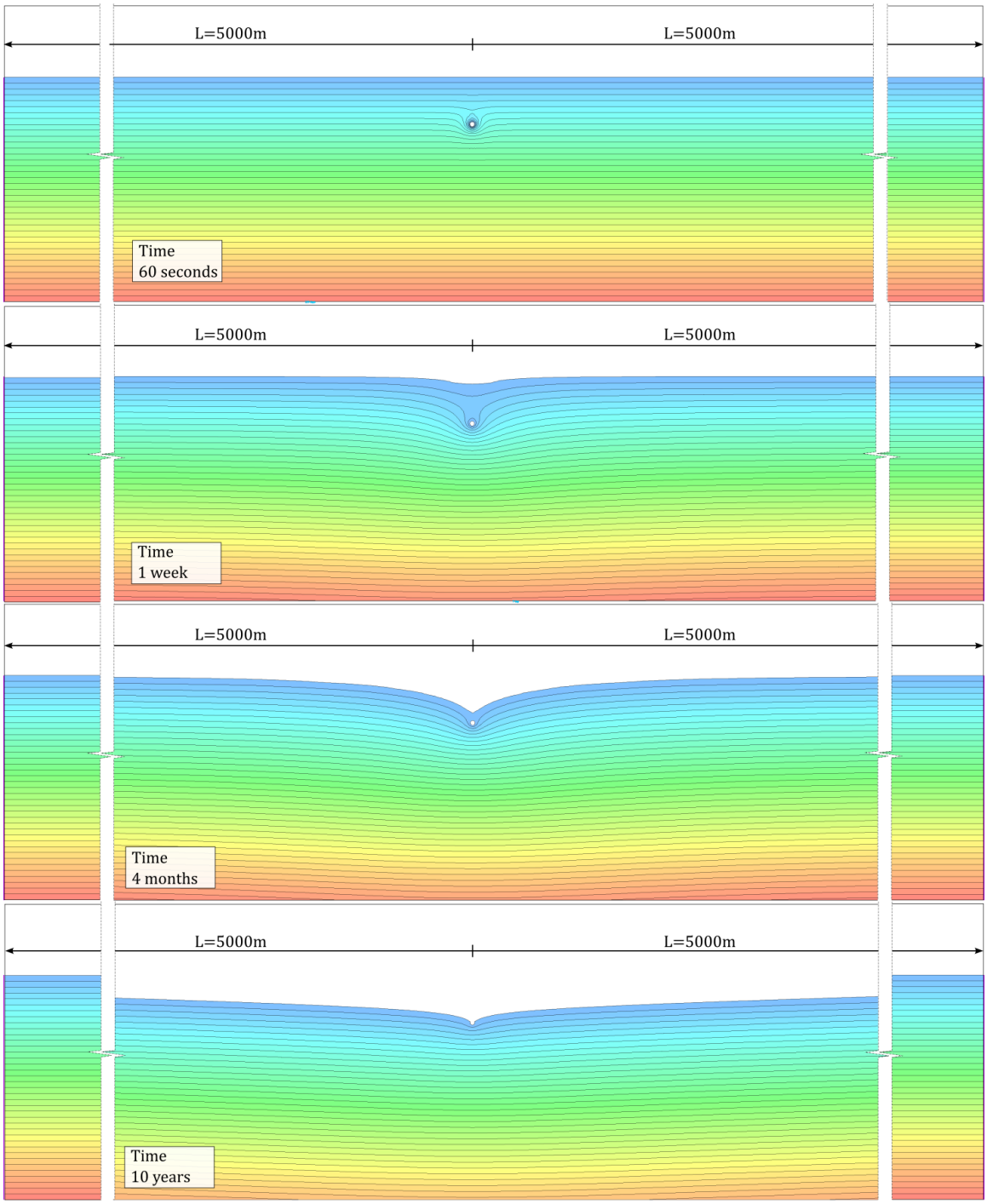

Figure 5 – Illustration of transient numerical simulation of constant lateral boundaries

Table 1 – Material parameters used in Figure 4

Case	Hydraulic conductivity	Porosity			Compressibility		
	k m/s	Saturated	Residual	Specific yield	Bulk Modulus (MPa)	m_v (1/kPa)	Specific storage (1/m)
Material 1	1×10^{-5}	0.25	0.005	0.245	3000	2.8×10^{-7}	4.0×10^{-6}
Material 2	1×10^{-6}	0.25	0.005	0.245	9000	8.3×10^{-8}	2.0×10^{-6}
Material 3	1×10^{-7}	0.25	0.005	0.245	10000	7.4×10^{-8}	2.0×10^{-6}
Material 4	1×10^{-8}	0.25	0.005	0.245	12000	6.2×10^{-8}	1.8×10^{-6}

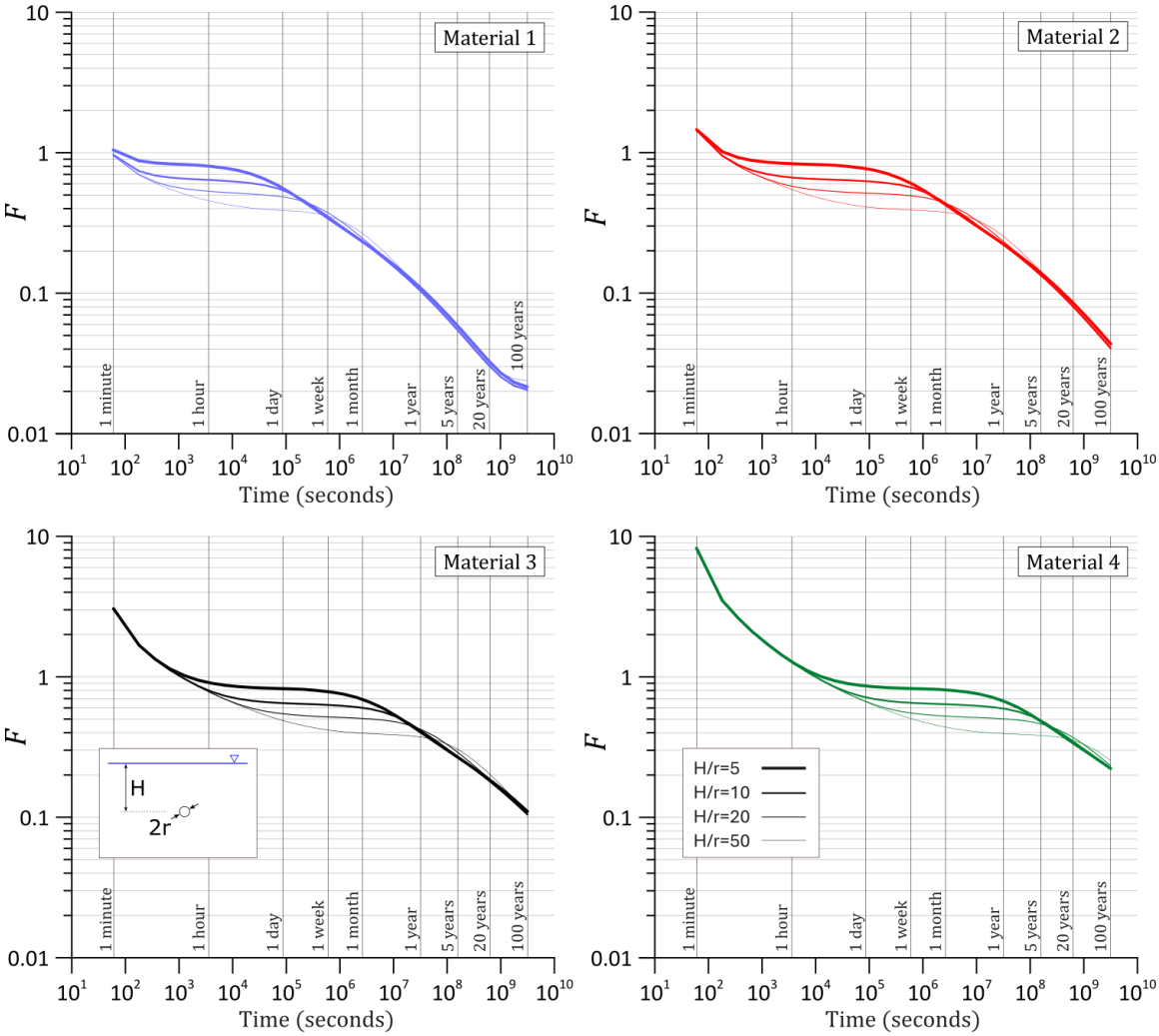

Figure 4– Shape factors for change in shape factor F (i.e., and inflows) over time

The rate of drawdown is a function of not only the hydraulic conductivity, but also the manner in which water is stored within the geology – where water may be released from draining the pore spaces (the 'specific yield' – a value similar to porosity) as well as decompression of the soil and rock matrix (the 'specific storage' – or its inverse its compressibility). It is the ratio of the hydraulic conductivity to storage (the "hydraulic diffusivity") that controls the rate of response. The values presented in Table 1 were selected to give a practical range of hydraulic diffusivity

values for reference. (It is also possible to reduce the curves of all 4 plots in Figure 4 to a single set of curves for all materials, by presenting the x-axis as the product of time and hydraulic diffusivity – whilst this is mathematically concise, such a plot is arguably less intuitive to use.) Values in Figure 5 pertain to a boundary some 5km from the tunnel and without representation of rainfall recharge. In practice, inflows may approach a steady state (i.e. F values flatten out with respect to time) in cases where a nearer boundary conditions apply.

SUMMARY

Analytical estimates of tunnel inflows using flownet analysis or published equations can be reduced to a shape factor. This allows simple and rapid comparison of inflow estimates for various tunnel design alternatives. The various plots of shape factors included above are presented as a useful reference to summarise various common approaches.

Published shape factors relate only to steady-state flows. The change of inflows over the life of a tunnel is often of interest, and shape factors derived from numerical transient analysis are presented for illustration and for reference.

Shape factors derived from flownets or analytical equations are typically only valid for specific geometries and idealised ground conditions. In modern practice, it is now relatively simple, and usually preferable, to make seepage estimates by using numerical modelling, which can facilitate representation of different geological units, heterogeneity, anisotropy and tailored boundary conditions. However, the large array of input variables used in modelling can complicate communication. The results of numerical modelling can be reduced back to a shape-factor to simplify and compare tunnel design alternatives and compare and validate inflow estimates.

REFERENCES

El Tani M. Water inflow into tunnels. In: Proceedings of the world tunnel congress ITA-AITES. Balkema: Oslo; 1999. p. 61–70.

Farhadian, H., Katibeh, H., 2017. New empirical model to evaluate groundwater flow into circular tunnel using multiple regression analysis. International Journal of Mining Science and Technology 27, 415–421. https://doi.org/10.1016/j.ijmst.2017.03.005

Goodman R, Moye D, Schalkwyk A, Javendel I. Groundwater inflow during tunnel driving. Eng Geol 1965;1:150–62.

Heuer RE. Estimating rock-tunnel water inflow. In: Proceeding of the rapid excavation and tunnelling conference.

Karlsrud K. Water control when tunnelling under urban areas in the Olso region. NFF Publ 2001;12(4):27–33.

Lei S. An analytical solution for steady flow into a tunnel. Ground Water 1999;37:23–6.

Raymer JH. Groundwater inflow into hard-rock tunnels: a new look at inflow equations. In: Rapid excavation and tunnelling conference. Seattle; 2005. p.457–68.